

10
7/11/95 g s (1)

Conf-950512--194

SLAC-PUB-95-6789
June 1995

A Final Focus System for the Next Linear Collider *

F. Zimmermann, K. Brown, P. Emma, R. Helm, J. Irwin, P. Tenenbaum, P. Wilson, Stanford Linear Accelerator Center, Stanford University, Stanford, CA 94309 USA

Abstract

The final focus of the Next Linear Collider (NLC) demagnifies electron and positron beams of 250–750 GeV energy down to a transverse size of about $2.5 \times 350 \text{ nm}^2$ at the interaction point (IP). The basic layout, momentum bandwidth, vibration tolerances, wakefield effects, and the tunability of the proposed final focus design are discussed. Also a perspective is given on the crab cavity and on effects of the solenoid field in the interaction region.

I. INTRODUCTION

The purpose of the NLC final focus system is to transport electron and positron beams at 500 GeV from the end of the big bend to the IP, where the demagnified beams are collided. The design spot size at the interaction point (IP) is about 2.5 nm vertically and 250–420 nm horizontally. The normalized emittances before collision are assumed to be as $\gamma\epsilon_x \approx 5 \times 10^{-6} \text{ m}$, $\gamma\epsilon_y \approx 5 \times 10^{-8} \text{ m}$, and the intra-bunch rms momentum spread as $\delta \approx 0.3\%$.

The entrance of the final focus system is formed by a skew-correction section (SCS) and a diagnostics section (DS) followed by a beta-matching section (BMS), horizontal and vertical chromatic correction sections (CCX and CCY), and the final transformer (FT). The final focus design is flexible enough to be operated at 500, as well as at 250 GeV. Furthermore, an upgrade to a beam energy of 750 GeV is possible. All data and figures in this report refer to the design for a 500 GeV beam energy, unless noted otherwise.

Table I lists important beam parameters at the interaction point. The luminosity may be doubled by reducing β_x^* to 10 mm. The minimum horizontal beta function at the IP will be determined by the maximum tolerable number of beamstrahlung photons and by the synchrotron radiation in the final doublet ('Oide effect' [8]).

Section II discusses the SCS. Section III presents two options for the DS. Section IV describes the BMS. The CCX, beta-exchanger (BX), CCY and FT are discussed in Section V. Section VI addresses the final doublet, and Section VII discusses the solenoid field and the crab cavity.

II. SKEW CORRECTION SECTION

The large emittance ratio of $\epsilon_x/\epsilon_y \approx 100$ in the NLC makes a dedicated SCS highly desirable. The SCS contains four *orthonormal* skew quadrupoles (i.e., they are orthogonal and equally scaled). Each of the four skew quadrupoles corrects one of the four beam correlations $\langle xy \rangle$, $\langle xy' \rangle$, $\langle x'y \rangle$,

*Work supported by Department of Energy contract DE-AC03-76SF00515.

Table I

Basic interaction-point beam parameters.

c.m. energy	1 TeV	comments
$L [\text{cm}^{-2} \text{s}^{-1}]$	$(2.7 \times 10^{34}) 1.3 \times 10^{34}$	Luminosity
N_b	1.1×10^{10}	Particles per bunch
n_b	90	Number of bunches
f	120 Hz	Bunch trains per s
H_D	1.32	Enhancement factor
σ_x	(220) 420 nm	variable
σ_y	2.5 nm	
β_x^*	(10) 37 mm	variable
β_y^*	100 μm	
ϵ_x	$5 \times 10^{-12} \text{ m}$	$\gamma\epsilon_x = 5 \times 10^{-6} \text{ m}$
ϵ_y	$5 \times 10^{-14} \text{ m}$	$\gamma\epsilon_y = 5 \times 10^{-8} \text{ m}$
$\sigma_{x',y'}$	(22) 12, 22 μrad	IP divergence
σ_z	100 μm	variable
θ_c	20 mrad	Crossing angle
δ_{rms}	3×10^{-3}	Energy spread
l^*	2 m	Free length from IP

and $\langle x'y' \rangle$. The first and second, and also the third and fourth, skew quadrupoles are separated by FODO cells with betatron phase advances of $\Delta\phi_{x,y} = \pi/2$ while the phase advances between the second and third are $\Delta\phi_x = \pi$, and $\Delta\phi_y = \pi/2$. The SCS is about 110 m long, and is able to correct a 300% emittance dilution due to linear coupling.

III. DIAGNOSTICS SECTION

The correctors of the SCS are adjusted based on emittance measurements in the DS, which is located immediately downstream. The projected emittances may be measured separately in the horizontal and vertical plane. Alternatively, the DS can be designed such that a four-dimensional measurement determines the two invariant emittances, as well as all four coupling parameters. The first, single-plane scheme would use four wire scanners (with two different wires—horizontal and vertical) separated by a phase advance of $\pi/4$. In this case, the DS is about 70 m long. The linear coupling is removed by minimizing the vertical projected emittance with each skew quadrupole of the SCS in turn. This procedure is invasive, has to be reiterated at least once, and may require several hours to perform. On the other hand, the fully-coupled scheme needs two additional wire scanners, as well as 45° wires on each scanner, and its length is about twice that of the single-plane scheme. This scheme allows a complete coupling measurement and correction within a few minutes, and could possibly be integrated into a feedback loop for automatic continuous decoupling.

MASTER

DISTRIBUTION OF THIS DOCUMENT IS UNLIMITED

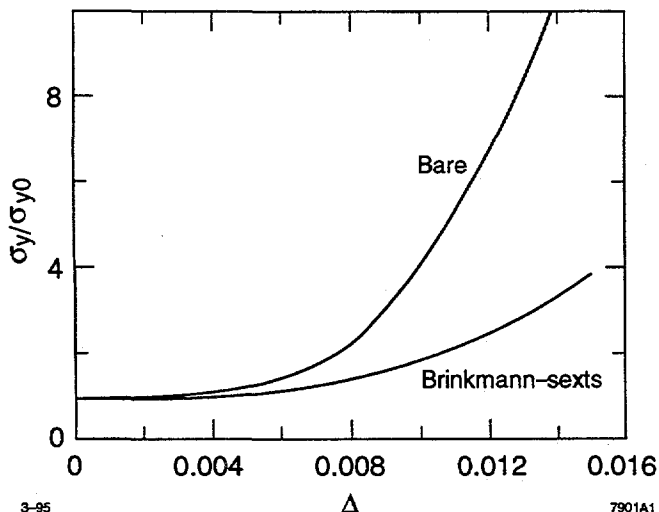


Figure. 1. Comparison of relative increase of vertical spot size with and without Brinkmann-sextupoles as a function of the half-width Δ of a uniform momentum distribution, for $\beta_x^* = 37$ mm and $\beta_y^* = 100$ μ m. Synchrotron radiation effects not included.

IV. BETA-MATCHING SECTION

The BMS is used to adapt the IP beta functions and the waist position to varying incoming beam conditions, and to adjust the phase advance between the collimator region and the IP. The BMS contains six quadrupoles and is 350 m long.

The magnification and waist positions can be verified at a pre-image of the IP located in the BX, where a sensitive beam size monitor, such as a laser-interferometer [1], will be installed. The energy spread is sufficiently large that, under normal operating conditions, the spot size at the pre-image is dominated by chromatic effects. Therefore, the strength of the main sextupoles in the CCX must be adjusted during tune-up, and only one plane can be measured at a time. The chromatically-corrected beam sizes at the pre-image are $\sigma_x \approx 1.4$ μ and $\sigma_y \approx 100$ nm.

A conventional wire scanner immediately upstream of the CCY, where the spot size is about 100 μ in both planes, serves as a 'divergence' monitor, which is used to determine the actual beta functions at the pre-image.

V. CCX, CCY AND FINAL TRANSFORMER

A. Layout

After the BMS the beam traverses CCX, BX, CCY, and FT. The CCX and the CCY contain sextupole pairs separated by a $-I$ transfer matrix to compensate for the chromaticity of the final doublet. The chromaticity between the two sextupoles of each pair, as well as inside the BX and in the FT, is locally compensated for by means of nine additional sextupoles at locations with nonzero dispersion, similar to those suggested by Brinkmann [2]. The local compensation increases the energy bandwidth by almost a factor of two (see Fig. 1).

The length of the final focus system of about 770 m was optimized by a procedure described in [3]. Orthogonal knobs similar to those suggested by Irwin for the SLC [4] provide

control over important terms in the beam-line Hamiltonian. The beam-based alignment of quadrupoles and sextupoles will be performed in the same way as in the SLC [5] or the FFTB [6].

B. Tolerances

B.1 Position Jitter and Ground Motion

The maximum tolerable incoming vertical orbit jitter is about $0.43 \sigma_y$, corresponding to a 2.3% loss of luminosity. An additional contribution to the position jitter at the IP from vibrations of magnets in the final focus (except for the final doublet) should be less than $0.1 \sigma_x$ or $0.2 \sigma_y$, which would be a further 0.5% luminosity reduction each. The tolerable incoherent vibration amplitudes for six magnets are then as small as 3 nm vertically and 25 nm horizontally.

These values are larger than typical ground motion amplitudes at frequencies above a few Hertz [7]. For lower frequency the amplitude of the ground motion increases, but is also better correlated over long distances [7]. At 1 Hz the tolerable ground-wave amplitude is about 5.5 nm. A feedback system will correct residual low-frequency orbit variations.

B.2 Dispersion

In addition to steering, displaced quadrupoles generate dispersion at the IP, both directly by the chromatic kick from the quadrupole and by the orbit-change in the downstream elements. The maximum tolerable dispersion at the IP is 150 nm, corresponding to a 2% blowup of the vertical spot size for an intrabunch energy spread of $\delta \approx 0.3\%$. Allocating a 2% luminosity loss to the magnets of the final focus, the tolerable vertical displacement is about 13 nm for the first two quadrupoles in the FT, 40 nm for the next upstream quadrupole, and 80 nm for the two quadrupoles in the center of the CCY. These tolerances correspond to an orbit change by about 100 nm at the center of the first doublet magnet, to be compared with a beam size of 40 μ . The horizontal displacement tolerances due to dispersion are 400 nm or larger. The relative field ripple of four CCX quadrupoles must be smaller than 5×10^{-4} , in order not to generate intolerable dispersion at the IP.

One possible way to control orbit and magnet drifts over several minutes with sufficient accuracy, is to integrate high-resolution rf BPMs (which measure nm orbit changes) into the structure of all quadrupoles. The measured orbits will be averaged over a subset for which the incoming orbit jitter is small, in order to detect slow drifts. Corrector magnets will then steer the orbit back to its nominal position.

A maximum tolerable value of 75 μ m for the second order dispersion at the IP translates into an absolute static vertical alignment tolerance, which is about 6 μ for the first two quadrupoles in the FT. A compensation scheme for this aberration will be necessary.

B.3 Skew Coupling and Waist Shift

The vibration tolerance for sextupole magnets is determined by the induced skew coupling and waist shift. A horizontal (vertical) vibration of the two main Y-sextupoles

DISCLAIMER

This report was prepared as an account of work sponsored by an agency of the United States Government. Neither the United States Government nor any agency thereof, nor any of their employees, makes any warranty, express or implied, or assumes any legal liability or responsibility for the accuracy, completeness, or usefulness of any information, apparatus, product, or process disclosed, or represents that its use would not infringe privately owned rights. Reference herein to any specific commercial product, process, or service by trade name, trademark, manufacturer, or otherwise does not necessarily constitute or imply its endorsement, recommendation, or favoring by the United States Government or any agency thereof. The views and opinions of authors expressed herein do not necessarily state or reflect those of the United States Government or any agency thereof.

DISCLAIMER

Portions of this document may be illegible in electronic image products. Images are produced from the best available original document.

by 160 nm (130 nm) causes a 2% luminosity loss. Skew coupling and waist shift is also generated by a displaced quadrupole in the CCX or CCY, which steers the orbit off-center through the next sextupole. For a few quadrupoles in the CCY, the vertical (horizontal) displacement tolerance due to this effect is 50 (150) nm. In addition, the relative stability of the bending magnets inside the CCY must be better than 5×10^{-6} or 2×10^{-5} , assuming a magnet string or independently fed magnets, respectively.

Finally, the relative quadrupole field ripple resulting in a 2% luminosity loss due to the induced waist shift is 3×10^{-5} or larger for all quadrupoles, except for the final doublet.

VI. FINAL DOUBLET

A. Steering Jitter Tolerance

The inner magnets (Q_1) of both final doublets are mounted inside a common barrel, which is supported at the magnet center. The tolerance on the relative vertical vibration of these two quadrupoles is 0.5 nm. The second quadrupole on either side (Q_2) has a separate support. For the Q_2 magnets, the maximum tolerable antisymmetric vibration amplitude is 1.4 nm.

B. Synchrotron Radiation

Oide's original formula [8] for the spot-size increase due to synchrotron radiation in the last quadrupole can be generalized to two planes (horizontal and vertical) and two quadrupoles (Q_1 and Q_2). The result is that a significant part of the vertical spot-size increase may be due to the focusing in the horizontal plane within Q_2 . This contribution gets smaller with increasing length of Q_2 . For $\beta_x^* = 25$ mm, the total vertical spot size increase due to synchrotron radiation in the proposed final doublet is about 2%. The Oide effect is enhanced by orbit jitter: a 1σ vertical-orbit change amplifies the increase of the rms spot size by a factor of 4, while the luminosity loss increases only by about a factor of 2 [9].

C. Wakefield

The resistive wakefield kick [10] inside the first magnet of the doublet, Q_1 , is significant. If the magnet is 3 m long and its inner radius 4.5 mm, the jitter amplification, $\Delta y'/\beta_y/\Delta y$, varies from 7.5 for a conductivity $\sigma = 10^6 \Omega^{-1} \text{ m}^{-1}$ to 0.75 for $\sigma = 10^{10} \Omega^{-1} \text{ m}^{-1}$. Here $\Delta y'$ is the resistive kick, β_y the vertical beta function, and Δy the beam centroid offset inside Q_1 . The effect of geometric wakefields is small.

VII. CRAB CAVITY AND SOLENOID

The two beams collide with a crossing angle of about 20 mrad. In order to align the bunches during collision, a crab cavity at the entrance to Q_2 provides a displacement with distance at the IP satisfying $\partial x^*/\partial z = \theta_C/2$, where θ_C is the crossing angle (about 20 mrad for the NLC). A 37.5 cm long X-band cavity requires a maximum voltage of 1.2 MV and an input power close to 250 kW.

The permissible voltage error for a 2% luminosity loss is about 6%. It is important that the phase difference between the two crab cavities is maintained to a very high precision, so that the two beams collide head on. The phase-difference jitter tolerance is 0.2 degree at X-band. If the two cavities are driven by the same klystron, one source of phase jitter is thermal changes of the transmission line. The temperature must be stable to $1/15^\circ \text{ C}$ in 0.2 s (or 20° C per minute). Assuming that the excitation of higher order modes is 10% of the induced fundamental mode, the alignment tolerance of the crab cavity from horizontal steering is 20 μm . The crab cavity phases with respect to beam arrival times, the crab cavity voltage and the alignment are monitored by feedback systems.

For a peak solenoidal field of 3 T, the maximum field perpendicular to the beam is 300 Gauss. The generator for the solenoid field is of the form $x^*p_y^*$, and is so large that it has to be compensated by one or two skew quadrupoles in front of the CCX (e.g., SCS) or close to the pre-image point. This generator is different from the ordinary $p_x^*p_y^*$ term that generates or corrects most of the skew coupling in the system. The solenoid will vertically steer the two beams in opposite direction by about 35 μ at the IP. The only way to correct this steering without generating an unacceptable dispersion is to displace Q_1 by about 20 μ . The residual dispersion of 9 μ can be corrected by displacing the incoming beam by 5 μ , which is tolerable in view of enhanced synchrotron radiation. Even for a crossing angle of 30 mrad, the spot size increase due to on-axis synchrotron radiation in the solenoid field is less than 1%.

VIII. SUMMARY

A design for an NLC final focus system at 1 TeV c.m. energy has been described. Based on SLC experience, strong emphasis was placed on tunability, redundant diagnostics, insensitivity to orbit-jitter, and upgrade potential. Some of the tolerances, such as those on the vibration of the final-doublet support barrel or on the phase-difference jitter for the two crab cavities, appear tight, but not hopeless.

References

- [1] T. Shintake, KEK-Preprint-94-129, 1994.
- [2] R. Brinkmann, DESY-M-90-14, 1990.
- [3] F. Zimmermann, R. Helm, J. Irwin, these proceedings 1995.
- [4] N.J. Walker, J. Irwin, M. Woodley, Proc. of PAC 93, Washington (1993); F. Zimmermann et al., these proceedings 1995.
- [5] P. Emma, Proc. of 3rd EPAC, Berlin, SLAC-PUB-5787, 1992.
- [6] P. Tenenbaum et al., SLAC-PUB-95-6769, 1995.
- [7] V. Juravlev et al., CERN-SL 93-53, 1993.
- [8] K. Oide, *Phys. Rev. Letters* 61 15, 1988, 1713.
- [9] K. Hirata, B. Zotter, K. Oide, *Phys. Lett. B* 224, 1989, 437.
- [10] J. Irwin et al. SLAC-PUB-5165, 1994.